

# Investigating Redundancy in Multimodal Large Language Models with Multiple Vision Encoders

Song Mao<sup>\*1</sup> Yang Chen<sup>\*1,2</sup> Pinglong Cai<sup>1</sup> Ding Wang<sup>1</sup> Guohang Yan<sup>1</sup> Zhi Yu<sup>2</sup> Botian Shi<sup>1</sup>

## Abstract

Multimodal Large Language Models (MLLMs) increasingly adopt multiple vision encoders to capture diverse visual information, ranging from coarse semantics to fine-grained details. While this approach is intended to enhance visual understanding capability, we observe that the performance gains from adding encoders often diminish and can even lead to performance degradation—a phenomenon we term *encoder redundancy*. This paper presents a systematic investigation into this issue. Through comprehensive ablation studies on state-of-the-art multi-encoder MLLMs, we empirically demonstrate that significant redundancy exists. To quantify each encoder’s unique contribution, we propose a principled metric: the Conditional Utilization Rate (CUR). Building on CUR, we introduce the Information Gap (IG) to capture the overall disparity in encoder utility within a model. Our experiments reveal that certain vision encoders contribute little—or even negatively—to overall performance, confirming substantial redundancy. Our experiments reveal that certain vision encoders contribute minimally—or even negatively—to the model’s performance, confirming the prevalence of redundancy. These findings highlight critical inefficiencies in current multi-encoder designs and establish that our proposed metrics can serve as valuable diagnostic tools for developing more efficient and effective multimodal architectures.

## 1. Introduction

Multimodal Large Language Models (MLLMs) have marked a significant leap in artificial intelligence, exhibiting

<sup>\*</sup>Equal contribution <sup>1</sup>Shanghai Artificial Intelligence Laboratory, Shanghai, China <sup>2</sup>Zhejiang University, Zhejiang, China. Correspondence to: Song Mao <maosong@pjlab.org.cn>.

*Proceedings of the 42<sup>nd</sup> International Conference on Machine Learning*, Vancouver, Canada. PMLR 267, 2025. Copyright 2025 by the author(s).

remarkable prowess in integrating visual and textual information for complex reasoning and generation tasks (OpenAI, 2025; DeepMind, 2025; Anthropic, 2024; Bai et al., 2025; Zhu et al., 2025). Their ability to interpret images, answer visual questions, and describe complex scenes has positioned them at the forefront of AI research.

A prominent architectural trend for enhancing their visual capabilities is the incorporation of multiple, distinct vision encoders. The rationale is intuitive: different encoders, potentially pre-trained with varied objectives or architectures, could capture complementary visual aspects—spanning global context (Radford et al., 2021; Zhai et al., 2023) to pixel-level details (Oquab et al., 2023; Kirillov et al., 2023), thereby providing a richer, more holistic representation to the language model (Tong et al., 2024b; Lu et al., 2024a; Jiang et al., 2024; Shi et al., 2024; Tong et al., 2024a; Li et al., 2024b). However, the assumption that *more encoders are always better* is proving to be overly simplistic. Emerging evidence suggests that performance gains from additional encoders are often marginal, and in some cases, models with more encoders underperform their counterparts with fewer (Shi et al., 2024; Fan et al., 2024). This counterintuitive outcome suggests a critical, yet underexplored, issue: *encoder redundancy*. This issue arises when multiple encoders provide overlapping or conflicting visual cues, forcing the model to either struggle with fusing these inputs or be distracted by irrelevant information. This leads not only to suboptimal performance but also to inefficient use of computational resources.

While significant research has focused on developing sophisticated fusion mechanisms for multi-encoder MLLMs, the fundamental question of whether and to what extent each encoder provides unique, non-redundant information remains largely unaddressed. This knowledge gap hinders our ability to design truly efficient and robust MLLMs. Motivated by this, our work seeks to answer three core research questions:

1. How prevalent is encoder redundancy in state-of-the-art multi-encoder MLLMs?
2. How can we quantitatively measure the individual contribution of each encoder and the overall level of redun-

dancy?

3. What architectural and training factors contribute to this redundancy?

To address these questions, we propose a novel analytical framework. First, we empirically demonstrate the presence of redundancy by systematically masking individual vision encoders in representative MLLMs (e.g., Eagle (Shi et al., 2024)) and measuring the impact on performance across a wide range of benchmarks. Second, to dissect encoder utility, we introduce the **Conditional Utilization Rate (CUR)**, a metric that quantifies the performance change attributable to a specific encoder given the presence of others. A low or negative CUR signals that an encoder is redundant or even detrimental. Building on this, we define the **Information Gap (IG)** as the difference between the maximum and minimum CUR values, which measures the heterogeneity of encoder contributions. A large IG signifies a substantial imbalance, highlighting a poorly optimized encoder set.

Our comprehensive experiments confirm that significant encoder redundancy is common in modern MLLMs. We find that model performance often degrades gracefully when encoders are removed, and in some cases, even improves. Our analysis reveals that certain encoders dominate performance on specific tasks (e.g., OCR), while others are largely interchangeable for more general VQA tasks. Furthermore, we find that factors such as naive feature fusion and the choice of frozen encoders can exacerbate redundancy. In summary, this paper makes the following contributions:

1. We provide the first systematic empirical study that validates the prevalence of encoder redundancy in multi-encoder MLLMs, identifying it as a critical factor limiting performance.
2. We introduce the Conditional Utilization Rate (CUR) and Information Gap (IG) as principled metrics to quantify individual encoder contribution and overall redundancy.
3. We investigate the factors that may cause encoder redundancy, which provides insights that can inform the design of more efficient and effective multi-encoder MLLM architectures, potentially guiding encoder selection or dynamic weighting strategies.

## 2. Related Work

### 2.1. Multimodal Large Language Models

The landscape of Multimodal Large Language Models (MLLMs) has evolved rapidly, with models demonstrating increasingly sophisticated capabilities in understanding and generating multimodal content. Early influential work

like Flamingo (Alayrac et al., 2022) pioneered the integration of pre-trained vision encoders and Large Language Models (LLMs) by introducing mechanisms like resamplers for token reduction and cross-attention layers for feature fusion. Subsequently, LLaVA (Liu et al., 2024) presented a simpler yet effective architecture consisting of a vision encoder, an LLM, and a projection layer, establishing a modular paradigm that facilitated scalability and adaptation. Efforts to enhance visual processing have included mPLUG’s (Li et al., 2022) visual abstractor for handling high-resolution inputs and InternVL’s (Chen et al., 2024b) dynamic aspect ratio matching. Similarly, Qwen-VL series (Wang et al., 2024a; Bai et al., 2025) introduced techniques like 2D-RoPE and M-RoPE to better model inter-modal relationships. These advancements underscore a continuous drive towards richer visual understanding and more effective vision-language alignment in MLLMs.

### 2.2. Employing Multiple Vision Encoders in MLLMs

Our research directly engages with the growing body of work on MLLMs that utilize a Mixture of Vision Encoders (MoVE), also referred to as multi-encoder MLLMs. The primary motivation behind MoVE architectures is to harness diverse visual features by combining encoders pre-trained with different objectives or on varied data. For instance, DeepSeek-VL (Lu et al., 2024a) integrates SigLIP (Zhai et al., 2023) for semantic understanding and SAM-B (Kirillov et al., 2023) for visual grounding. HiLight (Wang et al., 2024b), Mini-Gemini (Li et al., 2024b), and CogAgent (Hong et al., 2024) employ dual encoders to capture features at varying levels of granularity. Other models like SPHINX (Lin et al., 2023) and Cambrian1 (Tong et al., 2024a) have explored using up to four distinct encoders.

Several works have focused on the architectural aspects of fusing information from multiple encoders. I-MoF (Tong et al., 2024b) uses separate projection layers for its two encoders, while Vary (Haoran et al., 2023) extends the vocabulary to manage inputs from different visual sources. Prism (Liu et al., 2023b) utilizes an expert resampler for outputs from an ensemble of experts. CoMM (Jiang et al., 2024) investigated effective combinations, finding CLIP (Radford et al., 2021) and DINO (Oquab et al., 2023) to be potent, while noting that MAE (He et al., 2022) and DeiT (Touvron et al., 2021) performed less effectively as visual branches. More recently, CLIP-MOE (Zhang et al., 2024b) proposed a model-agnostic strategy for building CLIP with a mixture-of-experts approach.

While these studies have significantly advanced the capabilities of MLLMs, their primary focus has been on achieving state-of-the-art performance or enabling new functionalities. The critical question of encoder redundancy—i.e., the extent to which additional encoders provide unique, non-

overlapping information—has received less direct attention. Although works like Eagle (Shi et al., 2024) and Mousi (Fan et al., 2024) have reported diminishing returns, our work distinguishes itself by moving beyond observation to systematic quantification. We introduce a diagnostic framework with novel metrics (CUR and IG) to precisely measure the contribution of each component encoder, thereby enabling a deeper understanding of the efficiency and necessity of each one.

### 2.3. Reducing Redundancy

Another line of work focus on reducing the redundancy of visual information by compressing or reducing the visual tokens. LLaVA-HR (Luo et al., 2024) and Mini-Gemini (Li et al., 2024b) fuse vision tokens of high resolution inputs into low resolution one when design the model architecture. Honeybee (Cha et al., 2024), TokenPacker (Li et al., 2024a), and Deco (Yao et al., 2024) leverage convolutions, local attentions, and average pooling to down-sample the features of high resolution images. Attention scores between vision and instructions tokens are also used to reduce vision tokens, such as FastV (Chen et al., 2024a), VTW (Lin et al., 2025), and PDrop (Xing et al., 2024) .

Compared with existing works, which focus on reducing redundancy within the extracted visual tokens, our work aims to reveal that the choice of vision encoders themselves can introduce redundancy at a higher level of abstraction.

## 3. Methodology

This section details our formal approach to investigating encoder redundancy. We first define the multi-encoder MLLM architecture (Section 3.1), then introduce our proposed metrics for quantifying redundancy (Section 3.2), and finally outline our experimental setup (Section 3.3).

### 3.1. Problem Formulation

We consider MLLMs based on the prevalent “ViT-adapter-LLM” architecture (Liu et al., 2024; Bai et al., 2025; Zhu et al., 2025).

For a multi-encoder MLLM with a set of  $n$  vision encoders  $\mathcal{E}_n = \{E_1, \dots, E_n\}$  as depicted in Fig 1. Given an image  $I$  and a text prompt  $T$ , the model’s response  $Y$  is generated as:

$$Y = f_{\mathcal{E}_n}(I, T) \\ = \text{LLM}(\text{proj}(\text{fuze}(E_1(I), \dots, E_n(I)), T)), \quad (1)$$

where  $\text{fuze}$  is a strategy for combining features from the different encoders (e.g., concatenation (Lu et al., 2024a; Tong et al., 2024b; Shi et al., 2024), attention-based fusion (Li et al., 2024b)), and  $\text{proj}(\cdot)$  is a projection layer that aligns visual features with the LLM’s embedding space.

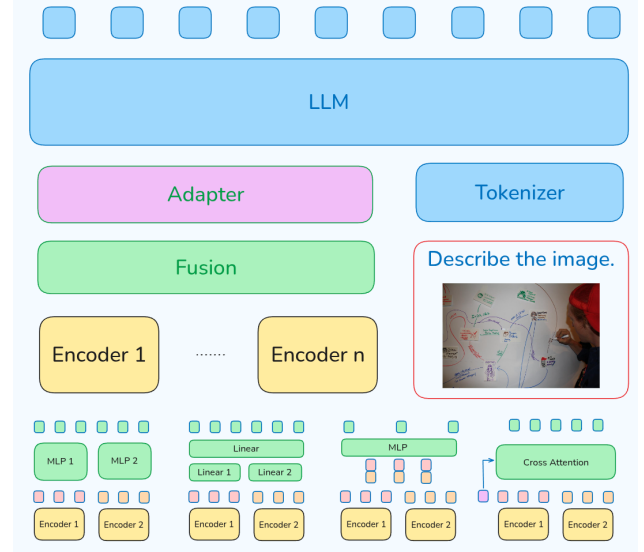


Figure 1. The architecture of multi-encoder MLLMs. (Top) Overall architecture, which consists of vision encoders, fusion layer, adapter and the LLM. (Down) Common fusion strategies to combine features from multiple vision encoders. Sequence append, shared MLP projection, Channel Concatenation, Cross-attention (from left to right).

While multiple encoders can theoretically provide more comprehensive visual information, they also risk introducing noise, conflicting signals, or, critically, redundant information. This redundancy can occur if encoders learn overlapping features or if some encoders provide information that is already provided by other encoders. We define encoder redundancy as a scenario where the inclusion of an encoder (or subset of encoders) does not lead to a meaningful performance improvement, or causes performance to degrade. More formally, encoder redundancy is observed if

$$\text{acc}(f_{\mathcal{E}_n}) \lesssim \max_{\mathcal{E}' \subsetneq \mathcal{E}_n} \text{acc}(f_{\mathcal{E}'}), \quad (2)$$

where  $\text{acc}(\cdot)$  is the model’s performance on a given benchmark, that is, removing one or several encoders will not harm or even improve the performance. Encoder redundancy suggests the information provided by that encoder is either already captured by others or introduces noise that the model cannot effectively resolve. We hypothesize that such counter-intuitive facts are often manifestations of significant underlying encoder redundancy. The additional computational cost and complexity of unused or detrimental encoders thus become unjustified.

### 3.2. Quantifying Encoder Contribution and Redundancy

To move beyond anecdotal observations, we introduce two metrics to quantify the utility of each encoder within a multi-encoder system.

**Conditional Utilization Rate (CUR)** To measure the unique contribution of an individual encoder  $E_i$  within the context of the full set  $\mathcal{E}_n$ , we define its Conditional Utilization Rate,  $u(E_i)$ , as the relative change in performance when  $E_i$  is ablated (masked):

$$u(E_i) = \frac{\text{acc}(f_{\mathcal{E}_n}) - \text{acc}(f_{\mathcal{E}_n \setminus \{E_i\}})}{\text{acc}(f_{\mathcal{E}_n})} \quad (3)$$

where  $f_{\mathcal{E}_n \setminus \{E_i\}}$  is the MLLM with encoder  $E_i$  masked (e.g., its output replaced by a zero tensor). The CUR,  $u(E_i)$ , quantifies the marginal utility of  $E_i$ . Since  $\text{acc}(\cdot) \in [0, 1]$ ,  $u(E_i)$  falls within  $(-\infty, 1]$ . A higher positive  $u(E_i)$  indicates that  $E_i$  provides a significant unique contribution. Conversely, a  $u(E_i)$  close to zero suggests that  $E_i$  is largely redundant, as its removal has little impact on performance. A negative  $u(E_i)$  indicates that the presence of  $E_i$  is detrimental, actively harming performance, potentially by introducing noisy or conflicting features.

**Information Gap (IG)** Building on CUR, we define the information gap,  $\Delta_{\text{gap},n}$ , for a set of  $n$  encoders as the difference between the maximum and minimum CUR values observed among them:

$$\Delta_{\text{gap},n}(\mathcal{E}_n) := \max_{i \in 1, \dots, n} u(E_i) - \min_{j \in 1, \dots, n} u(E_j). \quad (4)$$

The Information Gap serves as a measure of the heterogeneity in encoder contributions. A small  $\Delta_{\text{gap},n}$  might suggest that all encoders contribute somewhat equally (though not necessarily all positively or significantly). A large gap  $\Delta_{\text{gap},n}$ , particularly when  $\min_j u(E_j)$  is low or negative, highlights significant imbalance and redundancy: some encoders are crucial, while others are underutilized or even counterproductive. This disparity can point to inefficiencies in the multi-encoder design. For instance, if one encoder has a high CUR while others have CUR values near zero, the latter are largely redundant, and their inclusion unnecessarily increases model complexity.

These two metrics, CUR and IG, form the cornerstone of our analysis, allowing us to dissect the utility of individual encoders and characterize the overall level of redundancy within MoVE architectures.

### 3.3. Experimental Setup

Our experiments are designed to: (1) empirically validate the existence of encoder redundancy scenarios across different MLLM architectures, and (2) apply our proposed CUR

and IG metrics to quantify these phenomena. We investigate two representative multi-encoder MLLMs, each embodying different approaches to multi-encoder integration:

**Eagle** Eagle (Shi et al., 2024) represents MLLMs designed with a larger ensemble of encoders (typically 4 or 5), including CLIP (Radford et al., 2021), ConvNext (Liu et al., 2022), SAM (Kirillov et al., 2023), EVA (Fang et al., 2024), and Pix2Struct (Lee et al., 2023). Eagle primarily uses channel concatenation for fusion. Its architecture provides an excellent testbed for investigating redundancy in systems with many specialized encoders, allowing us to calculate CUR for each and assess the overall IG.

**Cambrian-1** Cambrian-1 (Tong et al., 2024a) introduces a vision-centric approach with a novel fusion mechanism called Spatial Vision Aggregator (SVA). SVA uses cross-attention with learnable queries to integrate features from multiple encoders, including CLIP (Radford et al., 2021), ConvNext (Liu et al., 2022), SigLIP (Zhai et al., 2023) and DINO (Oquab et al., 2023), rather than directly feeding all image tokens to the LLM. This offers a contrast to simpler concatenation methods and allows us to study if more sophisticated fusion can mitigate redundancy. We analyze reported performance and, where possible, conduct masking experiments based on its architecture.

**Evaluation Benchmarks** To assess MLLM performance and analyze redundancy across diverse capabilities, we adopt the benchmark categorization proposed by Cambrian-1 (Tong et al., 2024a). This framework groups common benchmarks into four distinct categories based on a principal component analysis of MLLM scores:

- **Chart & OCR:** Emphasizes text extraction and reasoning from visual documents (e.g., ChartQA, OCRBench, TextVQA, DocVQA).
- **Knowledge-based VQA:** Relies on world knowledge and complex reasoning integrated with visual perception (e.g., SQA, MMMU, MathVista, AI2D).
- **Vision-Centric Tasks:** Requires detailed visual understanding and focus on visual attributes (e.g., MMVP, RealWorldQA, CV-Bench 2D/3D).
- **General VQA:** Assesses overall comprehensive visual understanding and reasoning (e.g., MME, MMBench, SEED-Bench, GQA).

Using these categories (detailed in Appendix Table 3) allows for a nuanced understanding of how encoder redundancy might manifest differently depending on the task demands. All evaluations are performed using standardized protocols, primarily leveraging the VLMEvalKit (Duan et al., 2025) for consistency.



## 4. Experiment

Our empirical investigation is designed to first validate the existence and extent of vision encoder redundancy in state-of-the-art MLLMs in Section 4.1, and second, to analyze the key factors that contribute to this phenomenon in Section 4.2.

### 4.1. Evidence of Pervasive Encoder Redundancy

In this section, we systematically probe the multi-encoder systems to demonstrate that significant redundancy is an inherent characteristic of current architectures.

**Performance Resilience to Encoder Ablation.** To demonstrate that redundancy is a common characteristic, we systematically probe multi-encoder systems by evaluating all  $2^n$  possible encoder combinations for a model with  $n$  encoders. Fig 2 and Fig 3 show the distribution of overall scores for Eagle-X5-7B and Cambrian-1-8B, respectively, as a function of the number of ablated encoders.

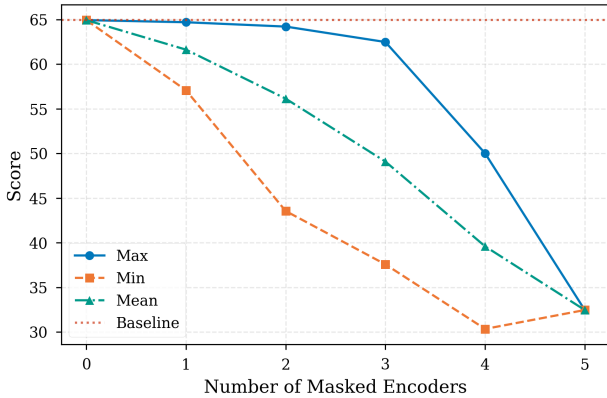


Figure 2. Score distribution of all possible combinations for Eagle-X5-7B

The results for both Eagle-X5-7B and Cambrian1-8B reveal a clear trend: performance degrades gracefully rather than catastrophically as encoders are removed. Both models exhibit remarkable resilience, maintaining high performance even with one or two encoders ablated. For Eagle-X5-7B, the best-case performance drops by less than 4% when masking three encoders. For Cambrian-1-8B, the optimal performance is achieved not with the full set of 4 encoders, but with a subset of 3. This gradual decline strongly suggests that the encoders provide partially overlapping information. The fact that removing an encoder can improve performance is a direct validation of our hypothesis.

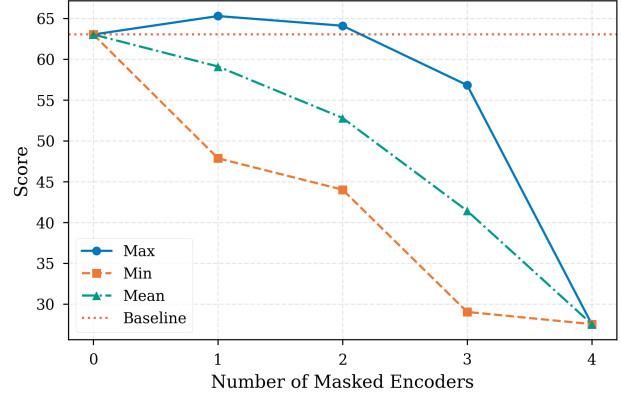


Figure 3. Score distribution of all possible combinations for Cambrian1-8B

**Finding 1:** Multi-encoder MLLMs exhibit significant redundancy. They can maintain a large fraction of their capabilities with a subset of their encoders, indicating that adding more encoders provides diminishing returns.

### Context-Dependent Utility and Negative Contributions.

We now apply our proposed metrics to dissect the unique contribution of each encoder. Tables 1 and 2 present the CUR and IG values for Eagle and Cambrian, respectively, across different task categories.

To dissect the contribution of each encoder, we analyze its impact conditioned on the presence of other encoders. For each encoder  $E_i$ , we compare the best and worst performance achieved across all subsets of encoders that *include*  $E_i$  against those that *exclude*  $E_i$ . Fig ?? and Fig ?? illustrate the results.

An ideal encoder would consistently improve performance, meaning the "Max Score with Encoder" (green dashed line) would always be above the "Max Score without Encoder" (green solid line). While this holds for some encoders like ConvNext, the results reveal a more complex reality. For instance, in Vision-Centric tasks, including the EVA encoder can lead to a lower maximum score than is achievable without it when other encoders are present. This indicates that its features, while potentially useful alone, can conflict with others. More strikingly, for some encoders and tasks, the minimum score with the encoder (red dashed line) is below the minimum score without it (red solid line), implying a net-negative contribution in certain contexts.

**Finding 2:** The contribution of a vision encoder is not absolute but highly context-dependent. Specific encoders can be detrimental to performance in certain combinations, suggesting that naive feature fusion can lead to "vision conflicts" that harm the model.

**Quantifying Specialization with CUR and IG.** We now employ our proposed metrics, Conditional Utilization Rate (CUR) and Information Gap (IG), to quantify the unique contribution of each encoder. Table 1 and Table 2 present the results for Eagle and Cambrian, respectively.

The data reveals differences in encoder utility across tasks.

1. **Task Specialization:** For specialized tasks like OCR & Chart, we observe extremely high IG values. In Cambrian-1, ConvNext achieves a CUR of 77.2%, indicating it provides indispensable, non-redundant information for this domain. Similarly, for Eagle-X5, the EVA encoder is dominant in Vision-Centric tasks.
2. **Redundancy in General Tasks:** In contrast, for Knowledge and General VQA, the IG values are much lower, and CURs are more evenly distributed. This suggests the encoders provide more homogeneous semantic features for these broad tasks, leading to higher redundancy where they are largely interchangeable.
3. **Negative Utility:** Notably, in Cambrian-1's Vision-Centric results, SigLIP exhibits a negative CUR (-16.16%), quantitatively confirming that its inclusion is actively harmful in that context, likely introducing conflicting signals that the fusion mechanism cannot resolve.

These results demonstrate that our CUR and IG metrics effectively quantify the severe imbalance in encoder contributions, moving beyond simple ablation to provide a more nuanced diagnostic picture.

**Finding 3:** Our CUR and IG metrics effectively quantify the severe imbalance in encoder contributions. Some encoders are highly specialized and indispensable for certain tasks (high CUR, high IG), while for other tasks, encoders are largely interchangeable and redundant (low CUR, low IG).

#### 4.2. Analyzing the Factors Driving Redundancy

Having established the existence of redundancy, we now investigate its underlying causes.

**The Role of Encoder Pre-training.** An encoder's pre-training objective is a primary determinant of its function within an MLLM. As seen in Table 1 and Table 2, encoders pre-trained for specific domains are least redundant when evaluated on those domains. The ImageNet-trained ConvNext is vital for OCR, just as the detection-focused EVA encoder excels in vision-centric tasks. In contrast, language-supervised (CLIP, SigLIP) and self-supervised (DINO) encoders provide broadly similar semantic features, making them more mutually redundant on general VQA tasks. This reveals a fundamental design trade-off: a set of diverse, specialized encoders may reduce redundancy but risks poor performance on general tasks where some encoders are underutilized.

**Fusion strategy.** The fusion strategy may also have an impact on the redundancy, Cambrian-1 uses SVA to cross-query all information extracted by different encoders. This do help the model to obtain more information, however, it also distract the model to pay attention to less important details, as a result, we identify a counterfactual fact: removing encoders improve the performance (Fig 3). As for channel concatenation, this strategy do not introduce learnable parameters and number of tokens. It put features in equal position, so from the result is more robust compared to Cambrian-1.

**Number of Vision Encoders.** The number of encoders should also be consider when studying encoder redundancy. Both Eagle (Shi et al., 2024) and MouSi (Fan et al., 2024) performs ablation study on number of encoders. According to MouSi, double encoders excels single encoder in most cases (8/9), when considering 3 encoders, the winning cases ratio drops to 4/6. Our experiment results shows a similar trend, that is, two encoders is a trade-off between performance and efficiency.

**Unfreezing Vision Encoders.** The method used to combine encoder outputs is paramount. A naive fusion strategy can fail to resolve conflicting features, exacerbating redundancy and even degrading performance. To demonstrate this, we conduct a controlled experiment on LLaVA-Next, augmenting the default CLIP encoder with a DINOv2 encoder. We fuse their patch embeddings using simple sequence appending (SA) or channel concatenation (CC).

The results are shown in Fig 4. On **General** and **Knowledge-based** benchmarks, both dual-encoder models perform substantially worse than the single-encoder (CLIP) baseline. This is a clear case of *vision conflict*: adding the DINOv2 encoder introduces features that, when naively fused, are not just redundant but actively detrimental. While marginal gains are observed for OCR and Vision-Centric tasks, this experiment underscores that without a sophisticated, learn-

Table 1. **CUR and IG of vision encoders in Eagle-X5-7B.** High IG values and disparate CURs in OCR & Chart and Vision-Centric tasks indicate strong specialization, while lower values in General and Knowledge tasks suggest higher redundancy.

CATEGORY	$n$	CLIP	CONVNEXT	SAM	EVA	PIX2STRUCT	AVG $\Delta_{gap,n}$
GENERAL	5	1.39%	1.94%	0.19%	10.08%	0.58%	9.89%
	4	4.1%	6.5%	0.92%	13.53%	2.18%	12.61%
	3	10.48%	13.31%	3.83%	18.64%	3.96%	14.81%
	2	22.8%	24.92%	13.86%	28.21%	12.6%	15.61%
KNOWLEDGE	5	1.82%	4.95%	1.1%	6.78%	2.04%	5.68%
	3	1.56%	4.53%	0.55%	5.94%	2.55%	5.38%
	3	3.53%	5.77%	2.01%	6.09%	3.7%	4.08%
	2	9.87%	10.61%	9.07%	9.98%	3.42%	7.2%
OCR & CHART	5	1.02%	30.26%	0.09%	13.34%	4.2%	30.17%
	4	6.47%	46.52%	2.93%	23.88%	22.29%	43.59%
	3	16.26%	54.86%	15.28%	28.16%	34.61%	39.58%
	2	42.01%	67.38%	40.16%	42.42%	45.86%	27.22%
VISION-CENTRIC	5	0.15%	2.54%	0.24%	17.34%	1.04%	17.19%
	4	3.16%	6.06%	1.72%	19.59%	3.08%	17.87%
	3	6.21%	8.68%	4.37%	19.13%	4.8%	14.76%
	2	9.41%	10.83%	7.95%	16.65%	7.75%	8.9%

Table 2. **CUR and IG of vision encoders in Cambrian-1 8B.** The table highlights the extreme specialization of ConvNext for OCR tasks (CUR up to 78%) and the detrimental effect of SigLIP in Vision-Centric tasks (negative CUR).

CATEGORY	$n$	CLIP	CONVNEXT	DINO	SIGLIP	AVG $\Delta_{gap,n}$
GENERAL	4	1.33%	1.15%	1.17%	-2.70%	4.03%
	3	7.01%	9.03%	2.02%	8.51%	7.00%
	2	27.78%	30.58%	14.39%	28.22%	16.19%
KNOWLEDGE	4	3.00%	11.29%	3.52%	-0.30%	11.59%
	3	2.66%	8.75%	1.45%	6.31%	7.31%
	2	5.34%	9.10%	4.09%	6.80%	5.00%
OCR & CHART	4	2.69%	74.98%	1.91%	3.02%	73.07%
	3	15.52%	77.20%	10.17%	15.26%	67.03%
	2	35.19%	78.09%	31.23%	35.18%	46.86%
VISION-CENTRIC	4	5.61%	1.43%	-1.38%	-16.16%	21.77%
	3	3.27%	2.74%	-0.80%	6.29%	7.08%
	2	16.40%	20.26%	9.86%	15.22%	10.41%

able fusion mechanism, adding more encoders can be counterproductive.

Fine-tuning encoders during instruction tuning, as done in Eagle and Cambrian, is a double-edged sword. It may allow encoders to specialize and reduce redundancy. However, it can also lead to *representational imbalance* (Huang et al., 2022), where the model learns to over-rely on a dominant encoder, effectively marginalizing the others and negating the benefits of a multi-encoder design.

**LLM Capacity.** Our investigation into the impact of model scale on encoder redundancy, as depicted in the Fig 5, reveals that while larger models achieves higher performance, they also exhibit the more significant redundancy. For instance, when a single encoder is masked on the 13B

model, performance can remain as high as 66.0% (a negligible drop from the baseline 67.0%) or plummet to 47.0%, depending on which encoder is removed. This wide variance, significantly larger than that observed in the 3B model, indicates a greater disparity in encoder contributions within the larger model. The largest model’s ability to maintain near-peak performance when its least important encoder is masked suggests a high degree of informational overlap. These findings strongly suggest that as LLM size increases, so does the propensity for encoder redundancy, making larger models more robust to the loss of some encoders but also highlighting greater inefficiency in their design.

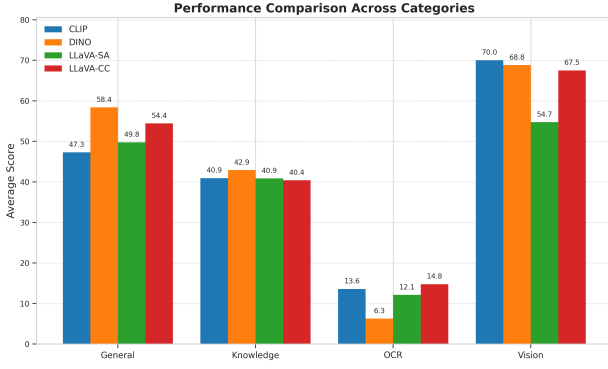


Figure 4. Performance of LLaVA-Next with single vs. multiple encoders. CLIP/DINO are single-encoder baselines. LLaVA-SA and LLaVA-CC are dual-encoder models. The performance drop in General and Knowledge tasks for dual-encoder models demonstrates that naive fusion can make additional encoders harmful, not just redundant.

## 5. Limitation and Conclusion

**Limitation** In this paper, we use the performance of MLLMs, that is,  $\text{acc}(\cdot)$  as the main metric, however, assessing MLLMs is not limited in its performance. The trustworthiness, robustness of MLLMs should also be considered, our definition of conditional utilization rate and information gap, which are based on task performance, may be inadequate for those dimensions. Though vision redundancy is observed in Eagle-X5-7B and Cambrian1-8B, it is still unclear whether this phenomenon arises in other multi-encoder MLLMs.

**Conclusion** In this paper, we conducted a systematic investigation into encoder redundancy in Multimodal Large Language Models. We identified and defined this phenomenon, where adding vision encoders yields diminishing or even negative returns. To analyze this issue quantitatively, we introduced two metrics: the Conditional Utilization Rate (CUR) to measure the marginal contribution of each encoder, and the Information Gap (IG) to quantify the overall disparity in their utility.

Our extensive experiments on state-of-the-art MLLMs validate the prevalence of significant encoder redundancy. We found that (1) MLLMs are surprisingly robust to encoder masking, indicating overlapping capabilities; (2) individual encoder contributions are highly task-dependent, with some encoders providing negligible or even detrimental signals; and (3) there is often a large information gap, with a few encoders dominating performance while others are underutilized.

These findings challenge the "more is better" assumption

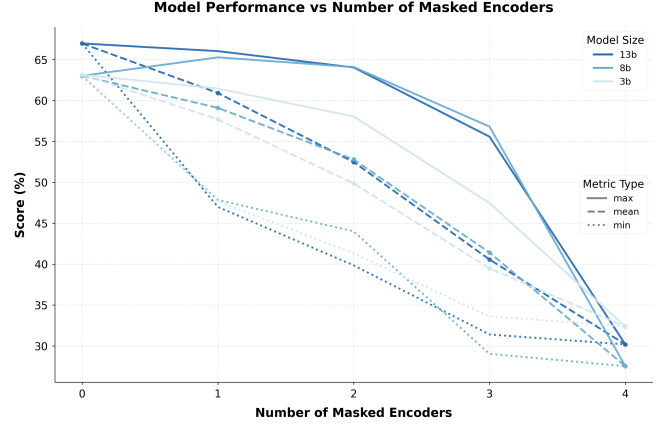


Figure 5. Performance against the number of masked encoders, with respect to 3B, 8B and 13B.

in MLLM design and provide a new analytical framework for diagnosing architectural inefficiencies. Our work opens several avenues for future research. The proposed metrics could guide the development of more parsimonious models through automated encoder selection or dynamic, context-aware weighting schemes. Furthermore, they could inform the design of more sophisticated fusion mechanisms that explicitly account for and mitigate potential redundancy. We hope this study paves the way for a more principled approach to building the visual systems of next-generation MLLMs.

## References

- Alayrac, J.-B., Donahue, J., Luc, P., Miech, A., Barr, I., Hasson, Y., Lenc, K., Mensch, A., Millican, K., Reynolds, M., et al. Flamingo: a visual language model for few-shot learning. *Advances in neural information processing systems*, 35:23716–23736, 2022.
- Anthropic. The claude 3 model family: Opus, sonnet, haiku. <https://www.anthropic.com>, 2024. URL [https://www-cdn.anthropic.com/de8ba9b01c9ab7cbabf5c33b80b7bbc618857627/Model\\_Card\\_Claude\\_3.pdf](https://www-cdn.anthropic.com/de8ba9b01c9ab7cbabf5c33b80b7bbc618857627/Model_Card_Claude_3.pdf).
- Azadani, M. N., Riddell, J., Sedwards, S., and Czarnecki, K. Leo: Boosting mixture of vision encoders for multimodal large language models, 2025. URL <https://arxiv.org/abs/2501.06986>.
- Bai, S., Chen, K., Liu, X., Wang, J., Ge, W., Song, S., Dang, K., Wang, P., Wang, S., Tang, J., et al. Qwen2.5-vl technical report. *arXiv preprint arXiv:2502.13923*, 2025.
- Cha, J., Kang, W., Mun, J., and Roh, B. Honeybee: Locality-enhanced projector for multimodal llm. In *Proceedings*



- of the *IEEE/CVF Conference on Computer Vision and Pattern Recognition (CVPR)*, 2024.
- Chen, L., Zhao, H., Liu, T., Bai, S., Lin, J., Zhou, C., and Chang, B. An image is worth 1/2 tokens after layer 2: Plug-and-play inference acceleration for large vision-language models, 2024a.
- Chen, Z., Wu, J., Wang, W., Su, W., Chen, G., Xing, S., Zhong, M., Zhang, Q., Zhu, X., Lu, L., et al. Internvl: Scaling up vision foundation models and aligning for generic visual-linguistic tasks. In *Proceedings of the IEEE/CVF Conference on Computer Vision and Pattern Recognition*, pp. 24185–24198, 2024b.
- DeepMind. Gemini 2.5 pro. <https://deepmind.google/technologies/gemini/pro/>, 2025.
- Duan, H., Fang, X., Yang, J., Zhao, X., Qiao, Y., Li, M., Agarwal, A., Chen, Z., Chen, L., Liu, Y., Ma, Y., Sun, H., Zhang, Y., Lu, S., Wong, T. H., Wang, W., Zhou, P., Li, X., Fu, C., Cui, J., Dong, X., Zang, Y., Zhang, P., Wang, J., Lin, D., and Chen, K. Vlmevalkit: An open-source toolkit for evaluating large multi-modality models, 2025. URL <https://arxiv.org/abs/2407.11691>.
- Fan, X., Ji, T., Jiang, C., Li, S., Jin, S., Song, S., Wang, J., Hong, B., Chen, L., Zheng, G., Zhang, M., Huang-caishuang, Zheng, R., Xi, Z., Zhou, Y., Dou, S., Ye, J., Yan, H., Gui, T., Zhang, Q., Qiu, X., Huang, X., Wu, Z., and Jiang, Y.-G. Poly-visual-expert vision-language models. In *First Conference on Language Modeling*, 2024. URL <https://openreview.net/forum?id=7QaEO9WYMa>.
- Fang, Y., Sun, Q., Wang, X., Huang, T., Wang, X., and Cao, Y. Eva-02: A visual representation for neon genesis. *Image and Vision Computing*, 149:105171, September 2024. ISSN 0262-8856. doi: 10.1016/j.imavis.2024.105171. URL <http://dx.doi.org/10.1016/j.imavis.2024.105171>.
- Fu, C., Chen, P., Shen, Y., Qin, Y., Zhang, M., Lin, X., Yang, J., Zheng, X., Li, K., Sun, X., Wu, Y., and Ji, R. Mme: A comprehensive evaluation benchmark for multimodal large language models, 2024. URL <https://arxiv.org/abs/2306.13394>.
- Ge, Y., Ge, Y., Zeng, Z., Wang, X., and Shan, Y. Planting a seed of vision in large language model. *arXiv preprint arXiv:2307.08041*, 2023.
- Haoran, W., Lingyu, K., Jinyue, C., Liang, Z., Zheng, G., Jinrong, Y., Jianjian, S., Chunrui, H., and Xiangyu, Z. Vary: Scaling up the vision vocabulary for large vision-language models. *arXiv preprint arXiv:2312.06109*, 2023.
- He, K., Chen, X., Xie, S., Li, Y., Dollár, P., and Girshick, R. Masked autoencoders are scalable vision learners. In *Proceedings of the IEEE/CVF conference on computer vision and pattern recognition*, pp. 16000–16009, 2022.
- Hiippala, T., Alikhani, M., Haverinen, J., Kalliokoski, T., Logacheva, E., Orekhova, S., Tuomainen, A., Stone, M., and Bateman, J. A. Ai2d-rst: A multimodal corpus of 1000 primary school science diagrams. *Language Resources and Evaluation*, 55:661–688, 2021.
- Hong, W., Wang, W., Lv, Q., Xu, J., Yu, W., Ji, J., Wang, Y., Wang, Z., Dong, Y., Ding, M., et al. Cogagent: A visual language model for gui agents. In *Proceedings of the IEEE/CVF Conference on Computer Vision and Pattern Recognition*, pp. 14281–14290, 2024.
- Huang, Y., Lin, J., Zhou, C., Yang, H., and Huang, L. Modality competition: What makes joint training of multi-modal network fail in deep learning? (Provably). In Chaudhuri, K., Jegelka, S., Song, L., Szepesvari, C., Niu, G., and Sabato, S. (eds.), *Proceedings of the 39th International Conference on Machine Learning*, volume 162 of *Proceedings of Machine Learning Research*, pp. 9226–9259. PMLR, 17–23 Jul 2022. URL <https://proceedings.mlr.press/v162/huang22e.html>.
- Hudson, D. A. and Manning, C. D. Gqa: A new dataset for real-world visual reasoning and compositional question answering. In *CVPR*, 2019.
- Jiang, D., Liu, Y., Liu, S., ZHANG, X., Li, J., Xiong, H., and Tian, Q. From CLIP to DINO: Visual encoders shout in multi-modal large language models, 2024. URL <https://openreview.net/forum?id=syoLhUJmth>.
- Kar, O. F., Tonioni, A., Poklukur, P., Kulshrestha, A., Zamir, A., and Tombari, F. Brave: Broadening the visual encoding of vision-language models. *arXiv preprint arXiv:2404.07204*, 2024.
- Kirillov, A., Mintun, E., Ravi, N., Mao, H., Rolland, C., Gustafson, L., Xiao, T., Whitehead, S., Berg, A. C., Lo, W.-Y., et al. Segment anything. In *Proceedings of the IEEE/CVF International Conference on Computer Vision*, pp. 4015–4026, 2023.
- Lee, K., Joshi, M., Turc, I., Hu, H., Liu, F., Eisenschlos, J., Khandelwal, U., Shaw, P., Chang, M.-W., and Toutanova, K. Pix2struct: Screenshot parsing as pretraining for visual language understanding, 2023. URL <https://arxiv.org/abs/2210.03347>.
- Li, C., Xu, H., Tian, J., Wang, W., Yan, M., Bi, B., Ye, J., Chen, H., Xu, G., Cao, Z., et al. mplug: Effective and efficient vision-language learning by cross-modal skip-connections. *arXiv preprint arXiv:2205.12005*, 2022.

- Li, W., Yuan, Y., Liu, J., Tang, D., Wang, S., Qin, J., Zhu, J., and Zhang, L. Tokenpacker: Efficient visual projector for multimodal llm. *arXiv preprint arXiv:2407.02392*, 2024a.
- Li, Y., Zhang, Y., Wang, C., Zhong, Z., Chen, Y., Chu, R., Liu, S., and Jia, J. Mini-gemini: Mining the potential of multi-modality vision language models. *arXiv preprint arXiv:2403.18814*, 2024b.
- Li, Z., Chen, G., Liu, S., Wang, S., VS, V., Ji, Y., Lan, S., Zhang, H., Zhao, Y., Radhakrishnan, S., Chang, N., Sapra, K., Deshmukh, A. S., Rintamaki, T., Le, M., Karmanov, I., Voegtli, L., Fischer, P., Huang, D.-A., Roman, T., Lu, T., Alvarez, J. M., Catanzaro, B., Kautz, J., Tao, A., Liu, G., and Yu, Z. Eagle 2: Building post-training data strategies from scratch for frontier vision-language models, 2025. URL <https://arxiv.org/abs/2501.14818>.
- Lin, Z., Liu, C., Zhang, R., Gao, P., Qiu, L., Xiao, H., Qiu, H., Lin, C., Shao, W., Chen, K., et al. Sphinx: The joint mixing of weights, tasks, and visual embeddings for multi-modal large language models. *arXiv preprint arXiv:2311.07575*, 2023.
- Lin, Z., Lin, M., Lin, L., and Ji, R. Boosting multimodal large language models with visual tokens withdrawal for rapid inference. In *Proceedings of the AAAI Conference on Artificial Intelligence*, volume 39, pp. 5334–5342, 2025.
- Liu, F., Eisenschlos, J., Piccinno, F., Krichene, S., Pang, C., Lee, K., Joshi, M., Chen, W., Collier, N., and Altun, Y. DePlot: One-shot visual language reasoning by plot-to-table translation. In Rogers, A., Boyd-Graber, J., and Okazaki, N. (eds.), *Findings of the Association for Computational Linguistics: ACL 2023*, pp. 10381–10399, Toronto, Canada, July 2023a. Association for Computational Linguistics. doi: 10.18653/v1/2023.findings-acl.660. URL <https://aclanthology.org/2023.findings-acl.660/>.
- Liu, H., Li, C., Wu, Q., and Lee, Y. J. Visual instruction tuning. *Advances in neural information processing systems*, 36, 2024.
- Liu, S., Fan, L., Johns, E., Yu, Z., Xiao, C., and Anandkumar, A. Prism: A vision-language model with multi-task experts. *arXiv preprint arXiv:2303.02506*, 2023b.
- Liu, Y., Duan, H., Zhang, Y., Li, B., Zhang, S., Zhao, W., Yuan, Y., Wang, J., He, C., Liu, Z., et al. Mmbench: Is your multi-modal model an all-around player? *arXiv preprint arXiv:2307.06281*, 2023c.
- Liu, Y., Li, Z., Li, H., Yu, W., Huang, M., Peng, D., Liu, M., Chen, M., Li, C., Jin, L., et al. On the hidden mystery of ocr in large multimodal models. *arXiv preprint arXiv:2305.07895*, 2023d.
- Liu, Z., Mao, H., Wu, C.-Y., Feichtenhofer, C., Darrell, T., and Xie, S. A convnet for the 2020s. *Proceedings of the IEEE/CVF Conference on Computer Vision and Pattern Recognition (CVPR)*, 2022.
- Lu, H., Liu, W., Zhang, B., Wang, B., Dong, K., Liu, B., Sun, J., Ren, T., Li, Z., Sun, Y., et al. Deepseek-vl: towards real-world vision-language understanding. *arXiv preprint arXiv:2403.05525*, 2024a.
- Lu, P., Mishra, S., Xia, T., Qiu, L., Chang, K.-W., Zhu, S.-C., Tafjord, O., Clark, P., and Kalyan, A. Learn to explain: Multimodal reasoning via thought chains for science question answering. In *The 36th Conference on Neural Information Processing Systems (NeurIPS)*, 2022.
- Lu, P., Bansal, H., Xia, T., Liu, J., Li, C., Hajishirzi, H., Cheng, H., Chang, K.-W., Galley, M., and Gao, J. Mathvista: Evaluating mathematical reasoning of foundation models in visual contexts. In *International Conference on Learning Representations (ICLR)*, 2024b.
- Luo, G., Zhou, Y., Zhang, Y., Zheng, X., Sun, X., and Ji, R. Feast your eyes: Mixture-of-resolution adaptation for multimodal large language models. *arXiv preprint arXiv:2403.03003*, 2024.
- Masry, A., Long, D. X., Tan, J. Q., Joty, S., and Hoque, E. Chartqa: A benchmark for question answering about charts with visual and logical reasoning. In *ACL*, 2022.
- Mathew, M., Karatzas, D., and Jawahar, C. Docvqa: A dataset for vqa on document images. In *WACV*, 2021.
- OpenAI. Gpt-4o system card. <https://openai.com/index/gpt-4o-system-card/>, 2025.
- Oquab, M., Darcet, T., Moutakanni, T., Vo, H., Szafraniec, M., Khalidov, V., Fernandez, P., Haziza, D., Massa, F., El-Nouby, A., et al. Dinov2: Learning robust visual features without supervision. *arXiv preprint arXiv:2304.07193*, 2023.
- Radford, A., Kim, J. W., Hallacy, C., Ramesh, A., Goh, G., Agarwal, S., Sastry, G., Askell, A., Mishkin, P., Clark, J., Krueger, G., and Sutskever, I. Learning transferable visual models from natural language supervision. In *International Conference on Machine Learning*, 2021. URL <https://api.semanticscholar.org/CorpusID:231591445>.
- Shen, L., Chen, G., Shao, R., Guan, W., and Nie, L. Mome: Mixture of multimodal experts for generalist multimodal

- large language models. *arXiv preprint arXiv:2407.12709*, 2024.
- Shi, M., Liu, F., Wang, S., Liao, S., Radhakrishnan, S., Huang, D.-A., Yin, H., Sapra, K., Yacoob, Y., Shi, H., Catanzaro, B., Tao, A., Kautz, J., Yu, Z., and Liu, G. Eagle: Exploring the design space for multimodal llms with mixture of encoders. *arXiv:2408.15998*, 2024.
- Singh, A., Natarajan, V., Shah, M., Jiang, Y., Chen, X., Batra, D., Parikh, D., and Rohrbach, M. Towards vqa models that can read. In *CVPR*, 2019.
- Tong, S., Brown, E., Wu, P., Woo, S., Middepogu, M., Akula, S. C., Yang, J., Yang, S., Iyer, A., Pan, X., et al. Cambrian-1: A fully open, vision-centric exploration of multimodal llms. *arXiv preprint arXiv:2406.16860*, 2024a.
- Tong, S., Liu, Z., Zhai, Y., Ma, Y., LeCun, Y., and Xie, S. Eyes wide shut? exploring the visual shortcomings of multimodal llms. In *Proceedings of the IEEE/CVF Conference on Computer Vision and Pattern Recognition*, pp. 9568–9578, 2024b.
- Touvron, H., Cord, M., Douze, M., Massa, F., Sablayrolles, A., and Jégou, H. Training data-efficient image transformers & distillation through attention. In *International conference on machine learning*, pp. 10347–10357. PMLR, 2021.
- Wang, P., Bai, S., Tan, S., Wang, S., Fan, Z., Bai, J., Chen, K., Liu, X., Wang, J., Ge, W., Fan, Y., Dang, K., Du, M., Ren, X., Men, R., Liu, D., Zhou, C., Zhou, J., and Lin, J. Qwen2-vl: Enhancing vision-language model’s perception of the world at any resolution. *arXiv preprint arXiv:2409.12191*, 2024a.
- Wang, Z., Zhou, Q., Yang, K., Mao, Z. L., et al. Hilight: Technical report on the modern ai video language model. *arXiv preprint arXiv:2407.07325*, 2024b.
- Wei, H., Kong, L., Chen, J., Zhao, L., Ge, Z., Yang, J., Sun, J., Han, C., and Zhang, X. Vary: Scaling up the vision vocabulary for large vision-language models, 2023. URL <https://arxiv.org/abs/2312.06109>.
- xAI. grok, 2024. URL <https://x.ai/blog/grok-1.5v>.
- Xing, L., Huang, Q., Dong, X., Lu, J., Zhang, P., Zang, Y., Cao, Y., He, C., Wang, J., Wu, F., et al. Pyramid-drop: Accelerating your large vision-language models via pyramid visual redundancy reduction. *arXiv preprint arXiv:2410.17247*, 2024.
- Yao, L., Li, L., Ren, S., Wang, L., Liu, Y., Sun, X., and Hou, L. Deco: Decoupling token compression from semantic abstraction in multimodal large language models. *arXiv preprint arXiv:2405.20985*, 2024.
- Yue, X., Ni, Y., Zhang, K., Zheng, T., Liu, R., Zhang, G., Stevens, S., Jiang, D., Ren, W., Sun, Y., Wei, C., Yu, B., Yuan, R., Sun, R., Yin, M., Zheng, B., Yang, Z., Liu, Y., Huang, W., Sun, H., Su, Y., and Chen, W. Mmmu: A massive multi-discipline multimodal understanding and reasoning benchmark for expert agi. In *Proceedings of CVPR*, 2024.
- Zhai, X., Mustafa, B., Kolesnikov, A., and Beyer, L. Sigmoid loss for language image pre-training. In *Proceedings of the IEEE/CVF International Conference on Computer Vision*, pp. 11975–11986, 2023.
- Zhang, H., You, H., Dufter, P., Zhang, B., Chen, C., Chen, H.-Y., Fu, T.-J., Wang, W. Y., Chang, S.-F., Gan, Z., and Yang, Y. Ferret-v2: An improved baseline for referring and grounding with large language models. In *First Conference on Language Modeling*, 2024a. URL <https://openreview.net/forum?id=EEPBOB2Xww>.
- Zhang, J., Qu, X., Zhu, T., and Cheng, Y. Clip-moe: Towards building mixture of experts for clip with diversified multiplet upcycling, 2024b. URL <https://arxiv.org/abs/2409.19291>.
- Zhang, S., Xu, Y., Usuyama, N., Xu, H., Bagga, J., Tinn, R., Preston, S., Rao, R., Wei, M., Valluri, N., Wong, C., Tupini, A., Wang, Y., Mazzola, M., Shukla, S., Liden, L., Gao, J., Crabtree, A., Piening, B., Bifulco, C., Lungren, M. P., Naumann, T., Wang, S., and Poon, H. Biomedclip: a multimodal biomedical foundation model pretrained from fifteen million scientific image-text pairs, 2025. URL <https://arxiv.org/abs/2303.00915>.
- Zhu, J., Wang, W., Chen, Z., Liu, Z., Ye, S., Gu, L., Tian, H., Duan, Y., Su, W., Shao, J., Gao, Z., Cui, E., Wang, X., Cao, Y., Liu, Y., Wei, X., Zhang, H., Wang, H., Xu, W., Li, H., Wang, J., Deng, N., Li, S., He, Y., Jiang, T., Luo, J., Wang, Y., He, C., Shi, B., Zhang, X., Shao, W., He, J., Xiong, Y., Qu, W., Sun, P., Jiao, P., Lv, H., Wu, L., Zhang, K., Deng, H., Ge, J., Chen, K., Wang, L., Dou, M., Lu, L., Zhu, X., Lu, T., Lin, D., Qiao, Y., Dai, J., and Wang, W. Internvl3: Exploring advanced training and test-time recipes for open-source multimodal models, 2025. URL <https://arxiv.org/abs/2504.10479>.
- Zong, Z., Song, G., and Liu, Y. Detrs with collaborative hybrid assignments training. In *Proceedings of the IEEE/CVF international conference on computer vision*, pp. 6748–6758, 2023.
- Zong, Z., Ma, B., Shen, D., Song, G., Shao, H., Jiang, D., Li, H., and Liu, Y. Mova: Adapting mixture of vision experts to multimodal context. *arXiv preprint arXiv:2404.13046*, 2024.

## A. Benchmark and Evaluation details

For consistency, all benchmarks are evaluated via VLMEvalKit (Duan et al., 2025). For MME benchmark, we only report its perception score to be consistent with (Tong et al., 2024a). Before averaging, we divide the MME score by 20 and OCRBench score by 10. We use Qwen-Plus as judge model when there is a need. Other configurations are kept default.

Table 3. Benchmark details

CATEGORY	BENCHMARK	METRIC	REMARK
GENERAL	GQA (HUDSON & MANNING, 2019)	ACCURACY	
	MMB (LIU ET AL., 2023C)	ACCURACY	
	MME (FU ET AL., 2024)	SCORE	
	SEED-I (GE ET AL., 2023)	ACCURACY	
KNOWLEDGE	AI2D (HIIPPALA ET AL., 2021)	ACCURACY	
	MATHVISTA (LU ET AL., 2024B)	SCORE	
	SQA-I (LU ET AL., 2022)	ACCURACY	
	MMMU (YUE ET AL., 2024)	ACCURACY	
OCR & CHART	DocVQA (MATHEW ET AL., 2021)	ACCURACY	
	CHARTQA (MASRY ET AL., 2022)	ACCURACY	
	OCRBENCH (LIU ET AL., 2023D)	SCORE	
	TEXTVQA (SINGH ET AL., 2019)	ACCURACY	
VISION-CENTRIC	CV-BENCH (TONG ET AL., 2024A)	ACCURACY	
	MMVP (TONG ET AL., 2024B)	ACCURACY	
	REAL WORLD QA (XAI, 2024)	ACCURACY	

## B. Multi-encoder MLLMs summarization

A bunch of related works combines the information extracted by multiple vision encoders, we summarize the MLLMs with MoVE and their fusion strategies in Table 4.

## C. Experiment result Details



Table 4. Fusion strategy and vision encoders used by MLLMs with MoVE

MODEL	FUSION	CLIP	SiGLIP	CONVNEXT	DINOv2	PIX2STRUCT	EVA-02	SAM	ViT
CAMIRAN-I(TONG ET AL., 2024A)	SVA	YES	YES	YES	YES				
MINI-GEMINI(LI ET AL., 2024B)	ATT	YES		YES					
EAGLE-X4(SHI ET AL., 2024)	CC	YES		YES		YES	YES		
EAGLE-X5(SHI ET AL., 2024)	CC	YES		YES		YES	YES	YES	
EAGLE 2(LI ET AL., 2025)	CC		YES	YES					
MOUSI(FAN ET AL., 2024)	MLP					YES	YES	YES	
DEEPSEEK-VL(LU ET AL., 2024A)	CC		YES					YES	
BRAVE(KAR ET AL., 2024)	SA	YES	YES		YES		YES		YES
I-MoF(TONG ET AL., 2024B)	I-MoF	YES			YES				
SPHINX(LIN ET AL., 2023)	CC	YES		YES	YES				
MOME(SHEN ET AL., 2024)	MoLE	YES			YES	YES			
MoVA <sup>a</sup> (ZONG ET AL., 2024)	MoV	YES			YES	YES			
COMM(JIANG ET AL., 2024)	SA	YES			YES				
FERRET-V2(ZHANG ET AL., 2024A)	SA	YES			YES				
LLAVA-HR(LUO ET AL., 2024)	MRA	YES			YES				
LEO(LUO ET AL., 2024)	MLP							YES	YES <sup>b</sup>
LEO-MINI(AZADANI ET AL., 2025)	COTR	YES		YES			YES		

<sup>a</sup>MoVA also uses Co-DETR(Zong et al., 2023), Deplot(Liu et al., 2023a), Vary(Wei et al., 2023) and BiomedCLIP(Zhang et al., 2025)<sup>b</sup>LEO uses InternViT (Chen et al., 2024b), which is a variant of ViT

Table 5. Summary results for Cambrian1-8B with respect to #Masked Encoders, averaged on possible combinations.

#MASKED ENCODERS	GENERAL	KNOWLEDGE	OCR & CHART	VISION-CENTRIC	OVERALL
0 (BASELINE)	67.47	57.88	70.08	56.65	63.02
1	67.31 (-0.2%)	55.34 (-4.4%)	55.61 (-20.6%)	58.14 (+2.6%)	59.10 (-6.2%)
2	62.84 (-6.9%)	52.69 (-9.0%)	39.19 (-44.1%)	56.47 (-0.3%)	52.80 (-16.2%)
3	46.98 (-30.4%)	49.35 (-14.7%)	21.58 (-69.2%)	47.75 (-15.7%)	41.42 (-34.3%)
4	23.33 (-65.4%)	45.07 (-22.1%)	5.91 (-91.6%)	35.83 (-36.8%)	27.54 (-56.3%)

Table 6. Summary results for Eagle-X5-7B

#MASKED ENCODERS	GENERAL	KNOWLEDGE	OCR & CHART	VISION-CENTRIC	OVERALL
0 (BASELINE)	70.77	54.79	66.60	67.55	64.93
1	68.77 (-2.8%)	52.96 (-3.3%)	60.09 (-9.8%)	64.67 (-4.3%)	61.62 (-5.1%)
2	65.02 (-8.1%)	51.36 (-6.3%)	47.82 (-28.2%)	60.32 (-10.7%)	56.13 (-13.6%)
3	58.49 (-17.4%)	49.19 (-10.2%)	33.55 (-49.6%)	55.11 (-18.4%)	49.09 (-24.4%)
4	46.51 (-34.3%)	44.97 (-17.9%)	17.59 (-73.6%)	49.31 (-27.0%)	39.60 (-39.0%)
5	31.94 (-54.9%)	43.69 (-20.3%)	7.52 (-88.7%)	46.71 (-30.9%)	32.47 (-50.0%)

Table 7. Benchmark details for Eagle-X5-7B

#MASKED	MASKED ENCODERS					PERFORMANCE			
	CLIP	CONVNEXT	SAM	EVA	PIX2STRUCT	GENERAL	KNOWLEDGE	OCR & CHART	VISION-CENTRIC
0						70.77	54.79	66.60	67.54
1			YES	YES		<b>70.64</b>	<b>54.18</b>	<b>66.54</b>	67.38
					YES	63.63	51.07	57.71	55.83
		YES				70.36	53.67	63.80	66.84
2	YES					69.40	52.07	46.44	65.82
						69.79	53.79	65.92	<b>67.44</b>
			YES		YES	<b>70.21</b>	<b>53.78</b>	63.60	66.51
			YES	YES		63.07	50.73	57.46	54.82
			YES	YES	YES	61.65	49.62	44.58	52.92
3	YES				YES	68.97	52.40	62.05	65.97
	YES	YES				65.69	51.35	40.81	64.53
	YES			YES		59.24	51.14	55.92	52.68
		YES	YES			69.39	52.51	46.22	65.59
		YES	YES	YES		53.88	47.76	24.97	47.56
4	YES		YES			69.86	53.64	<b>66.01</b>	<b>67.29</b>
		YES			YES	68.22	50.62	16.53	65.29
	YES		YES		YES	<b>69.04</b>	<b>52.77</b>	<b>62.04</b>	<b>66.05</b>
	YES	YES			YES	64.97	47.96	10.84	62.91
	YES	YES		YES		33.39	45.85	27.33	43.71
5	YES	YES	YES			65.32	51.16	40.26	64.06
		YES		YES		53.07	47.50	24.73	46.84
			YES	YES	YES	61.13	49.26	44.19	51.84
	YES		YES	YES	YES	58.08	48.88	44.20	50.76
	YES		YES	YES		58.45	50.63	55.57	51.92
6		YES		YES	YES	53.27	47.25	10.07	47.59
		YES	YES		YES	68.17	50.63	16.25	65.39
	YES		YES	YES	YES	56.91	<b>48.95</b>	<b>44.18</b>	49.99
		YES	YES	YES	YES	51.94	47.47	10.13	46.87
	YES	YES	YES	YES		28.07	34.78	15.30	43.21
7	YES	YES		YES	YES	31.03	45.91	7.653	43.64
	YES	YES	YES		YES	<b>64.60</b>	47.70	10.68	<b>62.83</b>
	YES	YES	YES	YES	YES	31.93	43.69	7.521	46.70

Table 8. Benchmark details for Cambrian1-8B

#MASKED	MASKED ENCODERS				PERFORMANCE			
	CLIP	SIGLIP	DINO	CONVNEXT	GENERAL	KNOWLEDGE	OCR & CHART	VISION-CENTRIC
0					67.47	57.87	70.08	56.65
1	YES				66.57	56.13	68.19	53.47
		YES			<b>69.29</b>	<b>58.05</b>	67.96	<b>65.80</b>
				YES	66.69	51.34	17.53	55.84
2			YES		66.68	55.83	<b>68.74</b>	57.43
		YES		YES	60.05	48.98	10.70	57.53
	YES	YES			59.77	52.64	63.91	50.31
	YES			YES	59.35	50.89	10.62	55.16
	YES		YES		<b>68.63</b>	<b>58.08</b>	66.40	<b>63.24</b>
		YES	YES		64.91	53.92	<b>66.75</b>	55.61
			YES	YES	64.28	51.61	16.71	56.95
3	YES	YES	YES		<b>57.04</b>	<b>53.72</b>	<b>60.57</b>	<b>55.93</b>
	YES	YES		YES	26.52	45.81	5.486	38.30
		YES	YES	YES	51.75	47.78	10.14	49.39
	YES		YES	YES	52.58	50.10	10.13	47.38
4	YES	YES	YES	YES	23.33	45.06	5.914	35.83

Table 9. Impact of the size of LLM on encoder redundancy. Cambrian1-3B, 8B, 13B are used.

LLM	#MASKED	0	1	2	3	4
3B	MAX	63.14	61.47	58.04	47.47	32.38
	MIN	63.14	47.68	41.31	33.62	32.38
	MEAN	63.14	57.70	49.86	39.48	32.38
8B	MAX	63.02	65.28	64.09	56.81	27.53
	MIN	63.02	47.85	44.00	29.03	27.53
	MEAN	63.02	59.10	52.79	41.41	27.53
13B	MAX	66.98	66.04	64.04	55.58	30.18
	MIN	66.98	46.99	39.85	31.40	30.18
	MEAN	66.98	60.92	52.47	40.56	30.18